Desalination and Water Treatment
www.deswater.com

doi: 10.5004/dwt.2020.26024

201 (2020) 301–312
October

Evaluation of $[Zn(bim)_2(bdc)]_n$-MOF for adsorption of Cs^+ ions from aqueous solution using batch and fixed bed operations

Abdolreza Nilchi[a], Reza Saberi[b,*], Kamran Sepanloo[b], Omid Mehraban[c], Rohollah Ahangari[b]

[a]*Materials and Nuclear Research School, Nuclear Science and Technology Research Institute (NSTRI), Tehran, Iran, email: anilchi@aeoi.org.ir (A. Nilchi)*
[b]*Nuclear Science and Technology Research Institute (NSTRI), P.O. Box: 11365-8486, Tehran, Iran, Tel. +982188221128; emails: rsaberi@aeoi.org.ir (R. Saberi), ksepanloo@aeoi.org.ir (K. Sepanloo), rahangari@aeoi.org.ir (R. Ahangari)*
[c]*School of Chemistry, College of Science, University of Tehran, Tehran, Iran, email: omehraban@gmail.com (O. Mehraban)*

Received 19 June 2019; Accepted 20 April 2020

ABSTRACT

Metal-organic frameworks (MOFs) are porous network compounds that result from the reaction between a transition metal and organic ligands. In this work, cesium ions were removed by the use of a synthesized MOF, zinc benzimidazole *benzene dicarboxylic acid* $[Zn(bim)_2(bdc)]_n$ (ZBB) in aqueous solution. Removal of cesium ions occurred with an ion-exchange mechanism. Scanning electron microscopy, X-ray diffraction, Fourier-transform infrared spectroscopy, Brunauer–Emmett–Teller, and thermogravimetric analysis were used to characterize ZBB complex. Bach technique was used for adsorption experiments and the effect of pH, time, temperature, and adsorbent dosage were studied. The study of adsorption isotherms indicated that the sorption process best fits Langmuir isotherm. Radiation studies indicated that this synthesized MOF could be used in medium-active wastewaters treatment. The column experiments were also investigated in order to obtain the dynamic capacity of the adsorption process.

Keywords: Cesium removal; Adsorption; Batch and column studies; Ion exchanger; Metal-organic frameworks; $[Zn(bim)_2(bdc)]_n$

1. Introduction

The effective purification of fluid wastages, for example, nuclear waste effluents, is one of the serious environmental problems that must be discussed in coming years [1]. The main examples of these contaminants are radionuclides Cs(137), Sr(89) and La(138) [2]. These radionuclides release normally or accidentally in nuclear fission commodities [3].

Several methods have been reported for the removal of cesium from aqueous waste including inorganic ion exchangers [4], precipitation [5], membrane filtration (6), photochemical methods [7] and liquid extraction [8] to purge these kinds of wastes. Among these techniques, ion-exchanging which is low cost and eco-friendly strategy [9,10] has drawn much attention for Cs^+ adsorption due to several advantages like simplicity, performances, and selectivity especially when the concentration of the cation is low [4,11].

Various inorganic ion exchangers such as silicotitanates, metal oxides, hexacyanoferrates, zeolites, and sodium titanates are used in nuclear facilities for the sorption of heavy metal ions from nuclear waste effluents. However, the slow operation rate in column studies has been the deterrent factor for their large-scale uses [12]. On the other hand, the usage of organic ion-exchanger materials has been reduced

* Corresponding author.

because of decomposition and possibly the release of the radionuclides [13].

Metal-organic frameworks (MOFs) have demonstrated a critical task in the advancement of new water-soluble adsorbents due to their surface properties, which definitely like permeable microenvironment and adjustable pore size [14–16]. The structure of the MOF is comprised of metal-oxide bunches grafted by organic through covalent bonds [17]. The metals generally used for the synthesis of MOFs are Zn(III), Cu(II), Mg(II), Ca(II), Ln(III), Al(III), Co(II), Cd(II), Zr(IV), Ti(III), etc. [1].

MOFs have indicated the high specific surface area, appropriate pore size, huge pore volume, and extraordinary constant porosity compared with the customary adsorbents, which makes them an excellent choice for ion-exchanger systems [18].

In this study, zinc benzimidazole *benzene dicarboxylic acid* $[Zn(bim)_2(bdc)]_n$ (ZBB) a MOF ion exchanger with a compact formula of ZBB was synthesized and used for cesium removal from aqueous solutions. The prepared sorbent was characterized by scanning electron microscopy (SEM), Fourier-transform infrared spectroscopy (FTIR), thermogravimetric analysis (TGA), Brunauer–Emmett–Teller (BET), and X-ray diffraction (XRD). Several factors including isotherm models, adsorption kinetics, the influence of contact time, pH, and interfering cations on the adsorption process were studied. The equilibrium results correlated with Langmuir, Freundlich, and Temkin isotherms.

2. Materials and methods

2.1. Materials

All solvents and chemicals used in this work were of analytical grade and used without any purification. Benzimidazole (bim) and a 1,4-benzene dicarboxylic acid (H_2bdc) were purchased from Merck Research Laboratories (West Point, PA). Zinc acetate $Zn(OAc)_2{\cdot}3H_2O$, cesium chloride (CsCl), sodium hydroxide (NaOH), and hydrochloric acid (HCl) were purchased from Sigma-Aldrich (USA). Stock solutions of chemicals were prepared by dissolving 0.05 g CsCl in 1 L of distilled water.

2.2. Preparation of ZBB

Chang's method [19] was used in order to prepare the adsorbent. 21.9 (mg) $Zn(OAc)_2{\cdot}3H_2O$, 11.8 (mg) benzimidazole (bim), 16.6 (mg) H_2bdc, 10 (ml) of distilled water and 0.5 (ml) of NaOH (0.2 M) solution were added into a reactor and mixed for 35 min. The solution was kept for 72 min in the wet autoclaving with a temperature of 150°C and pressure of 6 bar. The mixture was kept at room temperature for 7 d after cooling at a rate of 2.5 (°C h^{-1}), finally, the crystalline shaped powder was obtained and stored for further uses.

2.3. Characterization of ZBB

Different devices used to characterize the synthesized MOF adsorbent. The BET surface area was carried out using a Quantachrome Nova2200e device (CHEMBET-3000 equipment American Quantachrome Company) characterizing functional groups of synthesized ZBB was carried out by meansof FTIR device (Jasco FT/IR 6600 spectrometer, Jasco, Tokyo, Japan). ZBB powder was mixed with KBr and the test carried out at wave number from 4,000 to 400 cm^{-1}. The surface morphology of the sorbent was determined by using scanning electron microscopy and obtained by the means of using the Zeiss-EVO 18 model at 25(kV) (Zeiss EVO 18, Germany). DSC-TGA, where TGA is thermogravimetry and DSC is differential scanning calorimeter, was done on the wet samples in the air with a heating rate of 10°C min^{-1} on DuPont model 951 (DuPont Instruments, Stevenage, UK).

3. Results and discussion

3.1. Characterization of synthesized MOF ZBB

3.1.1. Surface area, pore size and pore volume

The BET surface area of synthesized MOF adsorbent is shown in Table 1. The BET surface area of synthesized MOF was calculated to be 49.831 $m^2\ g^{-1}$.

3.1.2. Thermogravimetric analysis

In order to study the thermal behavior of the synthesized adsorbent, the TGA analysis of synthesized ZBB was carried out in the temperature range of 25°C–560°C and the result is shown in Fig. 1. As illustrated in Fig. 1, the weight reduction up to 120°C is due to evaporation of free water of ZBB samples and weight reduction up to 320°C is due to the elimination of water of crystallization in MOF samples. The last weight loss step occurs up to 540°C where structural decomposition of MOF samples occurs and the organic ligands decompose.

3.1.3. X-ray diffraction

In order to evaluate resistance to irradiation of the synthesized ZBB, three sets of samples including un-irradiated, irradiated up to 10 KGy, and irradiated up to 35 KGy were prepared and XRD analysis was carried out. Fig. 2 depicts the XRD pattern of un-irradiated (a), irradiated up to 10 KGy (b), and irradiated up to 35 KGy (c) of synthesized MOF. The analysis of XRD patterns revealed that the crystal structure of synthesized ZBB is resistant up to 10 KGy and at higher irradiation power, 35 KGy, The crystalline structure has disintegrated.

3.1.4. Fourier-transform infrared spectroscopy

The FTIR spectra of synthesized MOF and free benzimidazole [20] are given in Fig. 3, which shows the similarity of the spectrum of free benzimidazole and synthesized ZBB. The

Table 1
BET surface area of synthesized MOF adsorbent

Adsorbent	BET surface area ($m^2\ g^{-1}$)	BET pore size (nm)	BET pore volume ($cm^3\ g^{-1}$)
$[Zn(bim)_2(bdc)]_n$	49.831	2.745	0.058

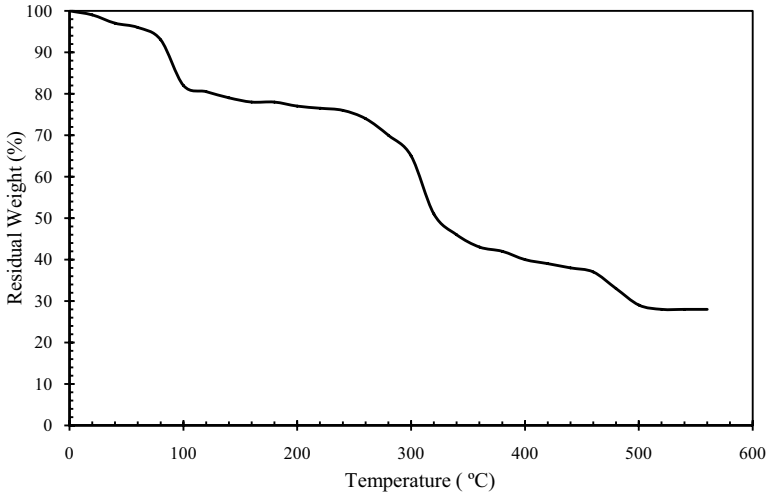

Fig. 1. TGA curve of the synthesized MOF adsorbent ZBB.

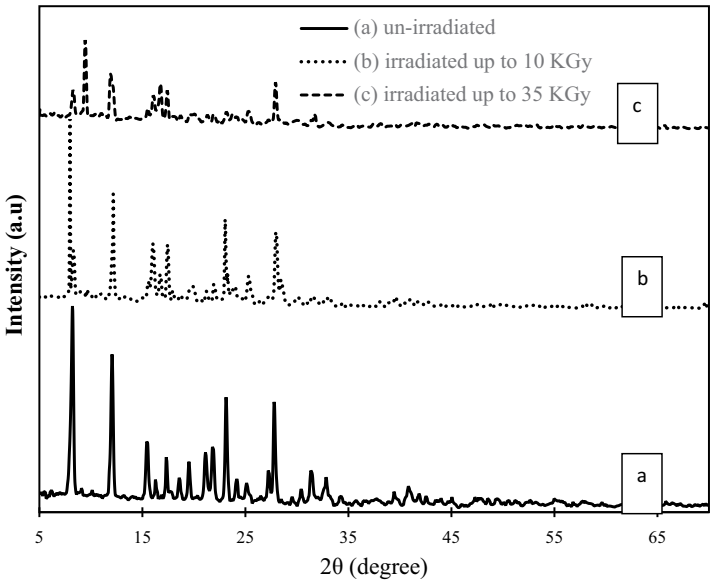

Fig. 2. XRD patterns of synthesized MOF (ZBB) (a) un-irradiated, (b) irradiated up to 10 KGy, and (c) irradiated up to 35 KGy.

peaks at 2,540; 3,075 and 3,360 cm^{-1} are related to stretch vibration of carboxyl (O–H), stretch vibration of carbon–hydrogen (C–H) bond in aromatic compounds and stretch vibration of (N–H) bond, respectively [21]. The peaks at 750 and 1,580 cm^{-1} correspond to bending vibration of (C–H) bonds, and bending vibration of C=C. The peak at 1,225 cm^{-1} correspond to the stretching vibration of (C–N) bonds [22] which is a typical signal of benzimidazole. The Zn–N stretch vibration has observed in 490 cm^{-1} that which is evidence of chelate coordination of ligand in the compound [23].

3.1.5. SEM image

SEM image of synthesized ZBB is shown in Fig. 4. The SEM image demonstrated surface morphology and size distribution of ZBB. As has been shown in Fig. 4, the size distribution of particles is homogenous and the average area of the particles is calculated to be 0.29 μm^2.

3.2. Effect of pH

pH of the medium is a standout amongst the most important factors influencing the Cs sorption action by the adsorbents [24]. Cesium (Cs^+) ions were in the form of ion in a wide range of solution pH due to no hydrolysis or forming complexes [25]. In order to discover the effect of initial solution pH, several batch experiments were carried out by adding 0.05 g of sorbent into 20 ml of Cs^+ solution with a concentration of 25 mg L^{-1} in the pH range of 1–13 at 25°C. Before adding sorbent, a specific amount of NaOH 0.5 N was added to the Cs^+ solution in order to reach the target pH. Each time before adding sorbent to the solution,

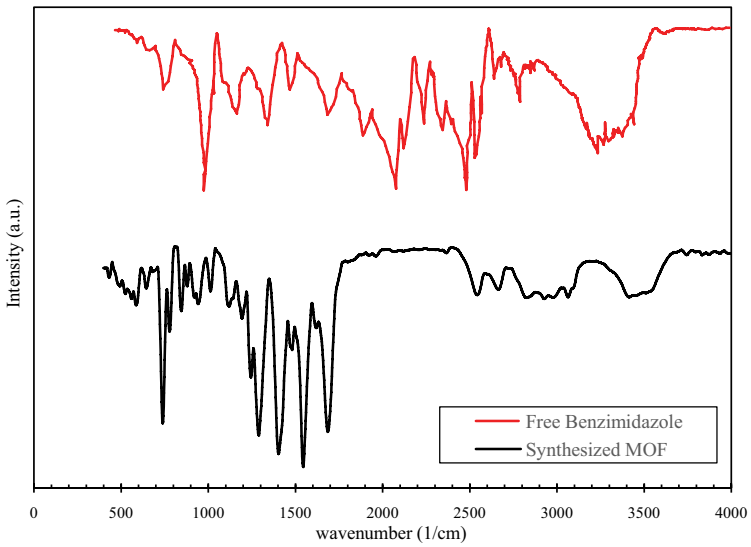

Fig. 3. FTIR spectra of free benzimidazole and synthesized MOF (ZBB).

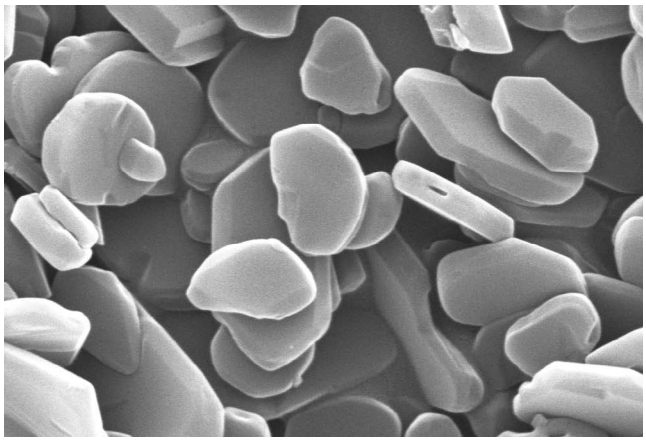

Fig. 4. Scanning electron microscopy (SEM) images of synthesized $[Zn(bim)_2(bdc)]_n$.

the Cs^+ solution was shaken at 100 rpm to homoenise the pH of the solution. Finally, after 10 min in order to separate solid from liquid, the suspension was centrifuged to isolate the solid phase from the liquid phase. The solution pH effect on percent uptake has defined with Eq. (1):

$$\%\ \text{uptake} = \frac{\left(C_0 - C_e\right)}{C_0} \cdot 100 \tag{1}$$

where C_0 and C_e are the primary and the equilibrium concentrations of the solution, respectively.

As shown in Fig. 5, sorption of Cs^+ ions has increased with increasing pH from 1 to 11. This behavior can be explained in such a way that in high acidity solutions competitions between H^+ and Cs^+ ions cause less sorption. In other words at higher pH values, the adsorbent surface had become deprotonated and interaction between surface and cation has increased [26,27]. After that at pH range 11–13, a slight decrease in sorption of Cs^+ ions can be seen. This is because adding NaOH solution might cause an increase in Na^+ ions that similar to H^+ ions and act as a competitor ion for Cs^+, which hinders the absorption of Cs^+ ions [3,27]. These results showed that ZBB has suitable sorption over a wide range of pH from 5.5 to 12.

3.3. Effect of time

In order to investigate the effect of sorbent contact time and find optimum contact time to reach maximum equilibrium, various studies were implemented. For this purpose, 0.05 g of the synthesized sorbent ZBB was equilibrated with 20 ml of 25(mg L^{-1}) cesium solution for different times of 10, 20, 30, 40, 50, 60, and 70 min. The amount of adsorbed Cs^+ per 1 g of the sorbent was calculated by the Eq. (2):

$$q_e = \left(C_0 - C_e\right) \cdot \frac{V}{M} \left(\text{mg/g}\right) \tag{2}$$

where V (L) is the solution volume and M (g) is the total amount of sorbent used for sorption study.

Time-dependent analyses for different time intervals were carried out. The result has been shown in Fig. 6. It is evident from the graph that the sorption process has reached equilibrium in 50 min with the q_e value of 9 mg g^{-1}. The swift initial stage is due to the high concentration gradient between the sorbent and solution. Fast absorption may lead to a decrease in the time required for removal, which minimizes operational cost [11,28,29].

The sorption kinetics of ZBB was investigated based on two kinetic sorption models: pseudo-first- and second-order models. Eqs. (3) and (4) demonstrate the linear forms of pseudo-first- and second-order models, respectively [30]:

$$\ln\left(q_e - q_t\right) = \ln q_e - K_1 t \tag{3}$$

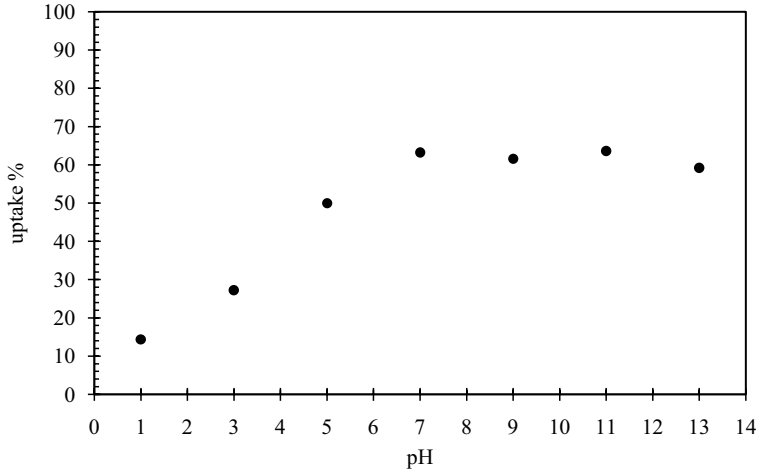

Fig. 5. Effect of pH on adsorption of Cs^+ ions.

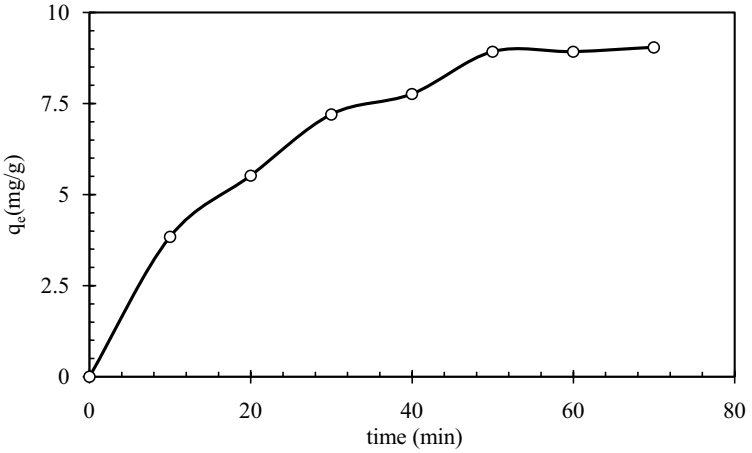

Fig. 6. Cesium sorption amount (q_e) on $[Zn(bim)_2(bdc)]_n$ adsorbent, as a function of time.

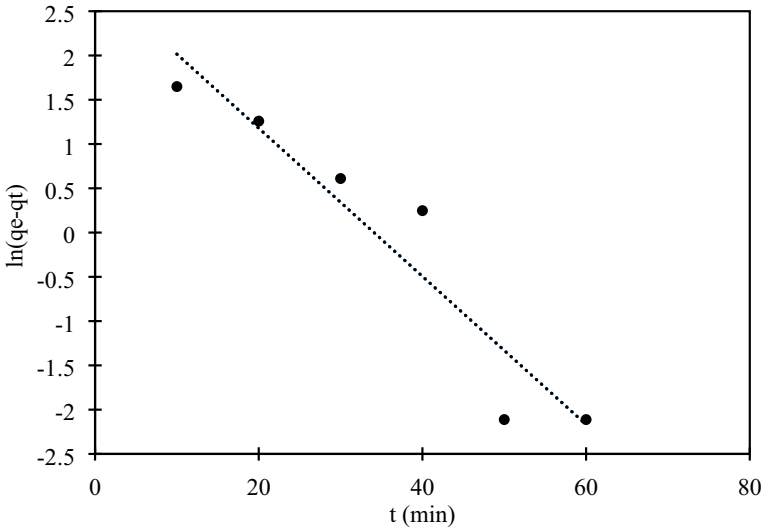

Fig. 7. Pseudo-first-order kinetic model for cesium sorption on $[Zn(bim)_2(bdc)]_n$ adsorbent.

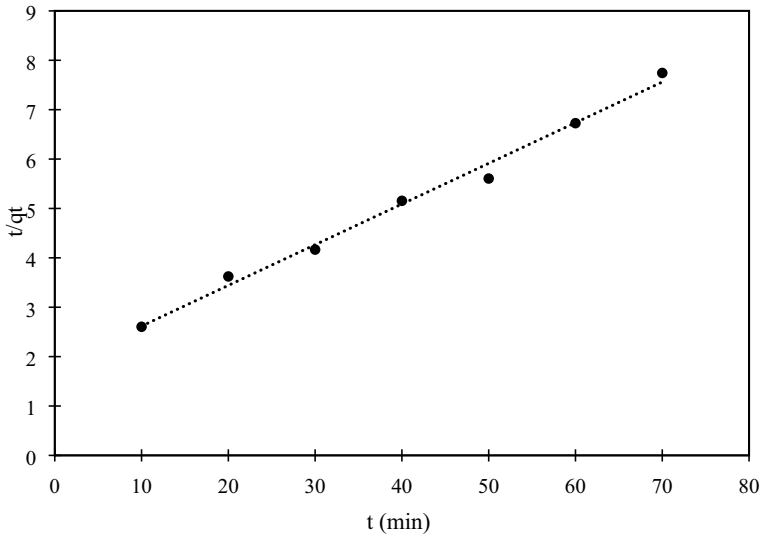

Fig. 8. Pseudo-second-order kinetic model for cesium sorption on $[Zn(bim)_2(bdc)]_n$ adsorbent.

$$\frac{t}{q_t} = \frac{1}{K_2 q_e^2} + \frac{t}{q_e} \quad (4)$$

where q_t and q_e are the the amount of solute sorbed per mass of sorbent (mg g^{-1}) at any time and equilibrium, respectively, and K_1 is the rate constant of first-order sorption (min^{-1}), and K_2 is the pseudo-second-order rate constant in g mg^{-1} min^{-1}. Table 2 shows the list of the parameters of the pseudo-first- and second-order models. It was also observed that calculated q_e from the pseudo-second-order model is more close to experimental q_e (9 mg g^{-1}), thus the pseudo-second-order model fits better to the sorption process that can be seen in Figs. 7 and 8.

3.4. Effect of adsorbent dosage

The effect of adsorbent dosages was studied for different amounts (0.05, 0.1, 0.15, 0.5, 1, and 2.5 g) of ZBB adsorbent in 20 ml of Cs^+ solution 25 (mg L^{-1}) at a temperature of 25°C, pH of 7, and contact time of 1 h as indicated in Fig. 11. As adsorbent weight increased the percent uptake increased and the adsorbent capacity decreased. This can be due to more available reactive sites on ZBB adsorbent [31,32]. Furthermore, the maximum adsorbent capacity (15.38 mg g^{-1}) was reported at 5 mg of nano-adsorbent, with uptake efficiency of 30.76%. On the other hand, with 2.5 g of nano-adsorbent, the maximum adsorption uptake obtained was 96.48% because of access to a substantial surface area, whereas adsorption capacity decreased to 3.71 mg g^{-1}.

3.5. Effect of temperature

In order to inquire about the impact of temperature on the sorption of Cs^+ radiocations (20 mg L^{-1}), various thermodynamic parameters were calculated. For this intent, six batch experiments at (25°C, 35°C, 45°C, 55°C, 65°C, and 75°C, pH 7 and contact time of 1 h) were accomplished. The thermodynamic parameters ($\Delta G°$, $\Delta S°$, and $\Delta H°$) were calculated by means of Eqs. (5)–(7) [33]:

$$K_d = \frac{q_e}{C_e} \quad (5)$$

$$\ln K_d^0 = \frac{\Delta S°}{R} - \frac{\Delta H°}{RT} \quad (6)$$

$$\Delta G° = -RT \ln K_d^0 \quad (7)$$

where K_d^0 is distribution coefficient (ml g^{-1}), q_e is the amount of Cs^+ adsorbed at equilibrium (mg g^{-1}), C_e is equilibrium concentration of (mg ml^{-1}), R is the universal gas constant (8.314 J mol^{-1} K^{-1}), $\Delta S°$ (J mol^{-1}), $\Delta H°$ (J mol^{-1}) and $\Delta G°$ (J mol^{-1}) changes in the entropy, enthalpy and Gibbs free energy for sorption process, respectively and T is the absolute temperature(K). The values of $\Delta H°$ and $\Delta S°$ were calculated with the slope and intercept of linear plot $\ln(K_d)$ vs. $1/T$ [33] are shown in Table 3. The obtained positive amount of $\Delta H°$ suggested that the sorption process is endothermic. On the other hand, a positive amount of $\Delta S°$ could be due to the liberation of more ions in the ions exchange process. Decreasing amounts of $\Delta G°$ that shown in Table 3 indicated that the ion-exchange process could be more spontaneous at higher temperatures. The effect of the solution temperature on the distribution coefficient of cesium ions on synthesized ZBB absorbant has been shown in Fig. 10.

3.6. Adsorption isotherms

Sorption isotherm models are typically used to acquire the connection between the concentrations of dissolved adsorbate in the aqueous solution and the amount of adsorbate on the solid phase at a constant pH and temperature [34]. Among sorption isotherm models Langmuir and Freundlich are the most well-known models. The Langmuir model based on assumption that a monolayer and homogenous adsorption occur on the surface of the adsorbent, while the

Table 2
Pseudo-first-order and pseudo-second-order parameters for cesium sorption on $[Zn(bim)_2(bdc)]_n$ adsorbent

Model	K_1 (mg g^{-1})	K_2 (g mg^{-1} min^{-1})	q_e (mg g^{-1})	R^2
Pseudo-first-order kinetic model	0.0837	–	17.31	0.90
Pseudo-second-order kinetic model	–	0.00378	12.13	0.99

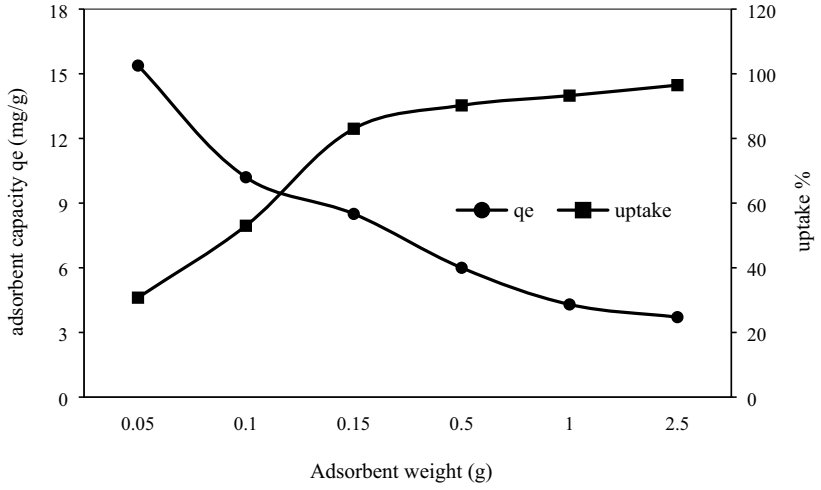

Fig. 9. Effect of adsorbent dosage on the adsorption of Cs^+ on ZBB.

Table 3
Thermodynamic parameters for the adsorption of Cs^+ onto the synthesized ZBB

Temperature (K)	$\Delta G°$ (kJ mol^{-1})	$\Delta H°$ (kJ mol^{-1})	$\Delta S°$ (J mol^{-1} K^{-1})
298.15	1.14	24.10	77.06
308.15	0.37	24.10	77.06
318.15	–0.39	24.10	77.06
328.15	–1.17	24.10	77.06
338.15	–1.93	24.10	77.06
348.15	–2.70	24.10	77.06

Freundlich model explains the sorption process as a multilayer and heterogeneous process [35].

3.6.1. Langmuir adsorption isotherm

The linearized type of Langmuir equation is given by Eq. (8) [35,36]:

$$\frac{C_e}{q_e} = \frac{1}{bq_m} + \frac{1}{q_m} C_e \tag{8}$$

where q_m is maximum monolayer sorption capacity (mg g^{-1}), b is the Langmuir coefficient (L mg^{-1}), C_e is the equilibrium cesium concentration and q_e is the amount of cesium adsorbed at equilibrium (mg g^{-1}). The Langmuir isotherm for sorption of Cs^+ ions is illustrated in Fig. 11. Table 4 showed the determined Langmuir parameters for adsorption of Cs^+ ions and the correlation correction value (R^2). The maximum monolayer sorption capacity (q_m), Langmuir coefficient, and the correlation correction value was found to be 80 mg g^{-1}, 0.0443 L mg^{-1}, and 0.985, respectively.

3.6.2. Freundlich adsorption isotherm

As previously explained the Freundlich isotherm model specifies the multiple-layer molecular adsorption process on the surface of the adsorbent. The parameter (1/n) indicates the desirability of the adsorbent for the ions. If the quantity of (1/n) is below 0.5 it indicates ease of the sorption process; if the quantity of (1/n) is above 2 it indicates that sorption is unfavorable for ions [37–39].

The linearized expression of Freundlich equation is given by Eq. (9) [40]:

$$\log\left(q_e\right) = \log\left(K_f\right) + \frac{1}{n}\log\left(C_e\right) \tag{9}$$

where K_f (mg g^{-1}) (L mg^{-1})$^{-1/n}$ and n are Freundlich constants related to adsorption capacity and intensity of adsorption, respectively. The Freundlich isotherm for sorption of Cs^+ ions is illustrated in Fig. 12. Table 5 showed the determined Freundlich parameters for adsorption of Cs^+ ions and the correlation correction value (R^2). The maximum multilayer sorption capacity (K_f), the intensity of adsorption, and correlation correction value was found to be 7.77 mg g^{-1} (L mg^{-1})$^{-1/n}$, 2.01 L mg^{-1} and 0.97, respectively. Meanwhile, (1/n) parameter was found to be 0.496 which indicates that the sorption process is favorable for cesium ions.

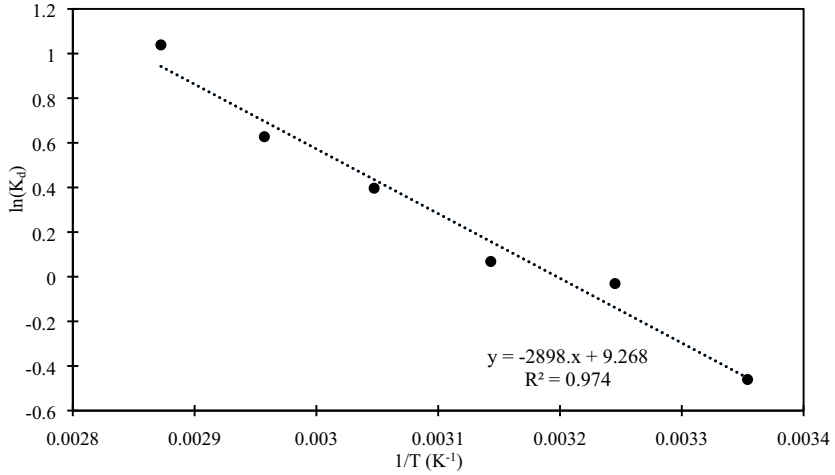

Fig. 10. Effect of solution temperature on the distribution coefficient of cesium ions on synthesized ZBB adsorbent.

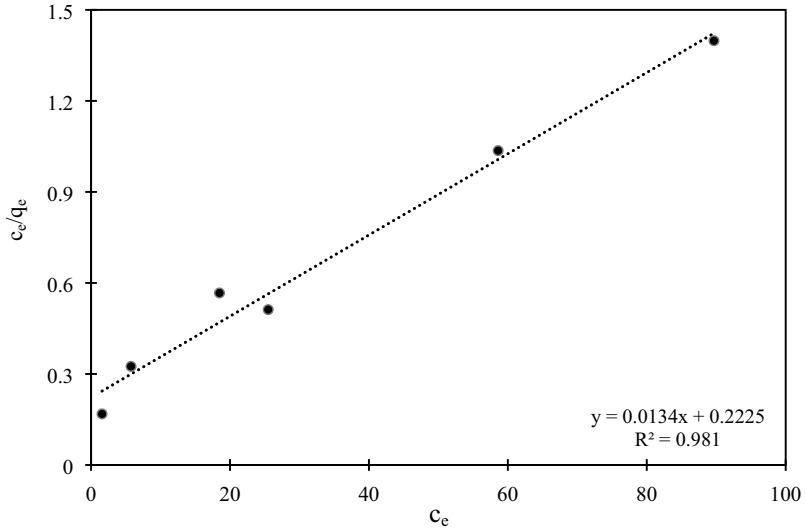

Fig. 11. Langmuir isotherm for adsorption of Cs^+ onto $[Zn(bim)_2(bdc)]_n$.

3.6.3. Temkin adsorption isotherm

Temkin isotherm is an adsorption model that presented to describe the adsorption of hydrogen on platinum anodes [40]. The deduction of the Temkin isotherm dependent on the supposition that the decrease of the heat of the sorption vs. temperature is linear [41]. The Temkin model is given by Eq. (10) [42]:

$$q_e = \left(\frac{RT}{b}\right) \times \ln\left(A \cdot C_e\right) \tag{10}$$

The linearized form of Temkin isotherm is given by Eq. (11) [43]:

$$q_e = \left(\frac{RT}{b}\right) \cdot \ln\left(A\right) + \left(\frac{RT}{b}\right) \ln\left(C_e\right) \tag{11}$$

Table 4
Langmuir parameters for adsorption of Cs^+ ions onto $[Zn(bim)_2(bdc)]_n$

Metal ion	Parameters for Langmuir model		
Cs^+	q_m (mg g^{-1})	b (L mg^{-1})	R^2
	80	0.0443	0.985

where q_e is the amount of adsorbed Cs^+ per 1 g of sorbent (mg g^{-1}), C_e is the equilibrium concentration of Cs^+ in the solution (mg L^{-1}), A is the Temkin isotherm equilibrium binding constant (L mg^{-1}), b is Temkin isotherm constant (J mol^{-1}), T is the absolute temperature (K), and R refers to universal gas constant (8.314 J mol^{-1} K^{-1}). Table 6 illustrates the determined Temkin parameters for the sorption of Cs^+ ions and the correlation correction value (R^2) the Temkin isotherm for

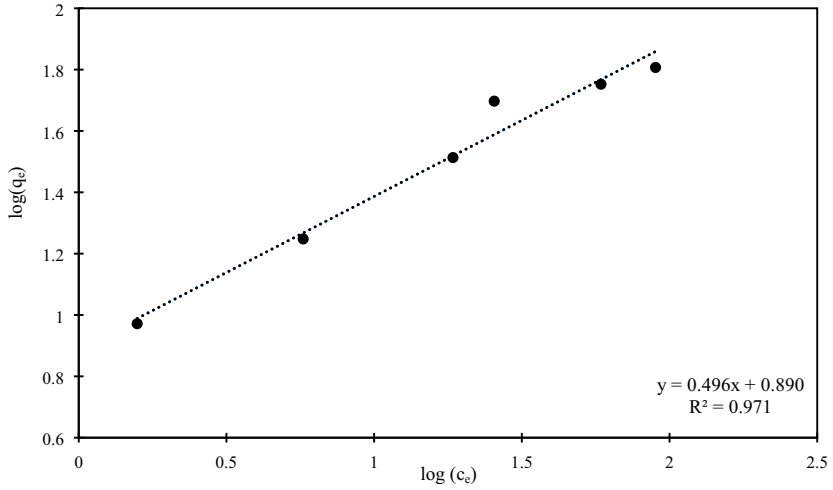

Fig. 12. Freundlich isotherm for adsorption of Cs^+ and onto $[Zn(bim)_2(bdc)]_n$.

Table 5
Freundlich parameters for adsorption of Cs^+ ions onto $[Zn(bim)_2(bdc)]_n$

Metal ion	Parameters for Freundlich model		
Cs^+	K_f (mg g^{-1})(L $mg^{-1})^{-1/n}$	n (L mg^{-1})	R^2
	7.77	2.01	0.97

Table 6
Temkin parameters for adsorption of Cs^+ ions onto synthesized ZBB

Metal ion	Parameters for Temkin model			
Cs^+	RT/b	b (J mol^{-1})	A (L mg^{-1})	R^2
	14.24	174.07	0.88	0.944

adsorption of Cs^+ and onto ZBB absorbant has been shown in Fig. 13.

3.7. Column studies

The flow in fixed bed sorption column is not at the equilibrium, thus isotherms cannot give accurate data for scale-up. Thus, it is important to carry out column experiments. A fixed bed column adsorption experiments was carried out to study the dynamic of cesium ions adsorption from aqueous solution by the synthesized MOF (ZBB). 0.05 g of synthesized ZBB sorbent was put in a glass tube with 0.8 cm diameter and 60 cm length. Later 200 ml of aqueous solution with a cesium concentration of 25 ppm were passed through the tube at a flow rate of 2 mL min^{-1}. The breakthrough curve was obtained by drawing C/C_0 curve against effluent volume, where C_0 is the initial concentration of cesium (25 ppm) and C is cesium concentration from the tube outlet. The cesium breakthrough curve of the

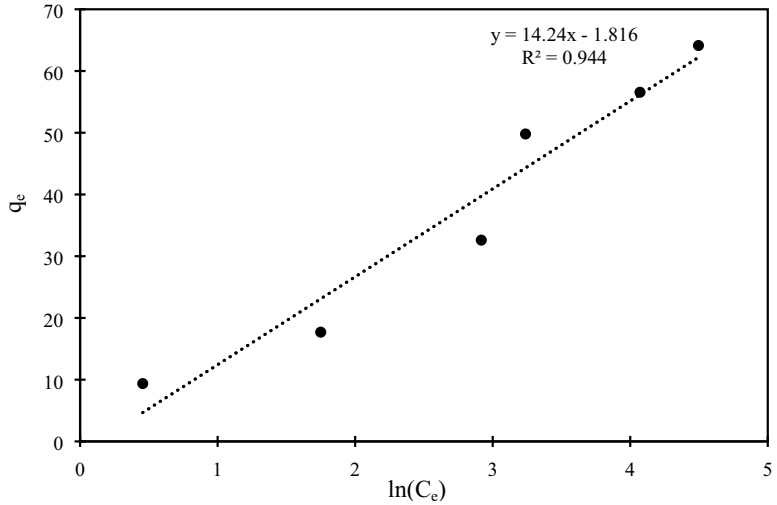

Fig. 13. Temkin isotherm for adsorption of Cs^+ and onto $[Zn(bim)_2(bdc)]_n$.

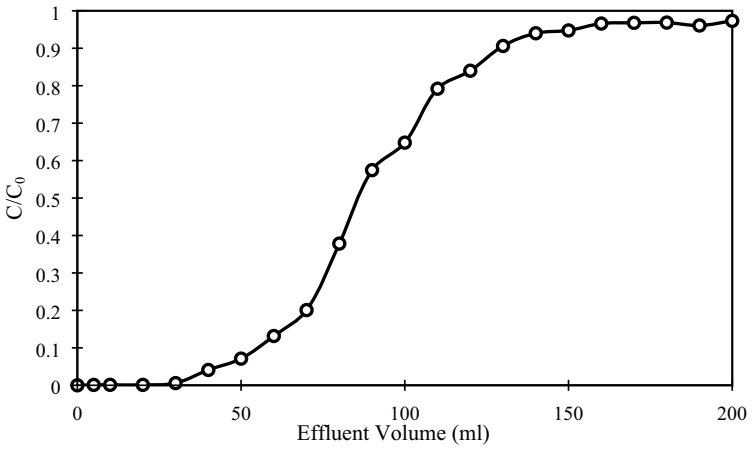

Fig. 14. The breakthrough curve of cesium on ZBB composite.

Table 7
Adsorption dynamic capacity in column experiment on ZBB adsorbent

Flow rate	Dynamic capacity at 5% breakthrough (practical)	Dynamic capacity at 100% breakthrough (total)	Efficiency of adsorbent column (%)
2 mL min^{-1}	21.22 mg Cs g^{-1} ZBB	57.95 mg Cs g^{-1} ZBB	36.58

ZBB ion exchanger is shown in Fig. 14. The breakthrough is defined as the point where the contaminated water concentration from the outlet of the column is about to 5%–10% of the initial contaminated water concentration [44].

To provide cesium dynamic adsorption capacity a second order kinetic equation was fitted to the data sets to throughput volume. This equation for Cs concentration was then submitted into the following relationship for dynamic capacity (DC) [45]:

$$\mathrm{DC} = \frac{\int_0^v (C_0 - C)dv}{M} \tag{12}$$

where v is the volume at breakthrough and M is mass of ZBB sorbent (g). Table 7 indicates that the DC at 5% and 100% breakthrough was found to be 21.22 and 57.95 mg g^{-1}, respectively. Also, Table 7 showed indicates that the efficiency of the adsorption column (E) can be calculated by Eq. (13) [45] was found to be 36.58%:

$$E = \frac{\text{area1}}{\text{area1} + \text{area2}} \tag{13}$$

where area1 is the area above the curve from C/C_0 = 0% till C/C_0 = 5%, and area2 is the area above the curve from C/C_0 = 5% to C/C_0 = 100%.

4. Conclusion

MOFs are a great choice for removing heavy metal ions because of their porous structures and ease in the synthesizing process. In this study, a synthesized MOF with the compact formula of ZBB was used to remove Cs^+ ion from nuclear effluents. Bach experiment with 0.05 g of adsorbent was performed to characterize the effect of temperature, time, pH, and adsorbent dosage. The pH of the solution has a critical effect on adsorption of cations. Experiments indicated that the maximum sorption occurs at a pH of 7. Adsorbent capacity was calculated to be 9 mg g^{-1} and the sorption process reached equilibrium within 50 min. With the presence of large amounts of H^+ and Na^+ ions, the sorption capacity of the synthesized sorbent has decreased. Equilibrium data revealed that Langmuir isotherm best fits with the sorption process. The calculated dynamic capacities for cesium were 21.22 and 57.95 mg Cs g^{-1} sorbent for 2 ml min^{-1} flow rate at 5% and 100% Cs breakthrough, respectively. Finally, the efficiency of the adsorption column was 36.58%.

Symbols

ZBB — $[Zn(bim)_2(bdc)]_n$
MOF — Metal-organic framework
bim — Benzimidazole
bdc — Benzene-1,4-dicarboxylic acid
Zn — Zinc
C_0 — Initial concentration of cesium
C_e — Equilibrium concentration of cesium
V — Volume
M — Mass of sorbent
q_e — Amount of adsorbed cesium at equilibrium
q_t — Amount of adsorbed cesium at time t
K_1 — Pseudo-first-order rate constant
K_2 — Pseudo-second-order rate constant

t — Time
K_d^0 — Distribution coefficient
R — Universal gas constant
ΔS — Change in the entropy
ΔH — Change in the enthalpy
ΔG — Change in the Gibbs free energy
T — Absolute temperature
b — Langmuir coefficient, Temkin isotherm constant
K_f — Freundlich constant related to adsorption capacity
n — Freundlich constant related to adsorption intensity
a — Temkin isotherm equilibrium binding constant
DC — Dynamic capacity

References

[1] P. Kumar, A. Pournara, K.-H. Kim, V. Bansal, S. Rapti, M.J. Manos, Metal-organic frameworks: challenges and opportunities for ion-exchange/sorption applications, Prog. Mater Sci., 86 (2017) 25–74.
[2] G.M. Naja, B. Volesky, Chapter 2 – Toxicity and Sources of Pb, Cd, Hg, Cr, As, and Radionuclides in the Environment, L.K. Wang, J.P. Chen, Y.-T. Hung, N.K. Shammas, Eds., Heavy Metals in the Environment, CRC Press, Taylor & Francis ebooks, London, 2009, pp. 14–58.
[3] A.M. El-Kamash, Evaluation of zeolite A for the sorptive removal of Cs^+ and Sr^{2+} ions from aqueous solutions using batch and fixed bed column operations, J. Hazard. Mater., 151 (2008) 432–445.
[4] B. Aguila, D. Banerjee, Z.M. Nie, Y.S. Shin, S.Q. Ma, P.K. Thallapally, Selective removal of cesium and strontium using porous frameworks from high level nuclear waste, Chem. Commun., 52 (2016) 5940–5942.
[5] T. Gäfvert, C. Ellmark, E. Holm, Removal of radionuclides at a waterworks, J. Environ. Radioact., 63 (2002) 105–115.
[6] D. Ding, Z. Zhang, R.Z. Chen, T.M. Cai, Selective removal of cesium by ammonium molybdophosphate – polyacrylonitrile bead and membrane, J. Hazard. Mater., 324 (2017) 753–761.
[7] F.H. Li, Y. Shang, Z.M. Ding, H.Q. Weng, J.X. Xiao, M.Z. Lin, Efficient extraction and separation of palladium (Pd) and ruthenium (Ru) from simulated HLLW by photoreduction, Sep. Purif. Technol., 182 (2017) 9–18.
[8] P.-Y. Chen, The assessment of removing strontium and cesium cations from aqueous solutions based on the combined methods of ionic liquid extraction and electrodeposition, Electrochim. Acta, 52 (2007) 5484–5492.
[9] A. Bhatnagar, M. Sillanpää, Utilization of agro-industrial and municipal waste materials as potential adsorbents for water treatment—a review, Chem. Eng., 157 (2010) 277–296.
[10] T. Bond, E.H. Goslan, S.A. Parsons, B. Jefferson, Disinfection by-product formation of natural organic matter surrogates and treatment by coagulation, MIEX and nanofiltration, Water Res., 44 (2010) 1645–1653.
[11] F. Ardestani, A. Haghighi Asl, T. Yousefi, M. Torab-Mostaedi, Impregnated of C_6CoFeN_6 nanoparticles in poly-1-naphthol for uptake of Cs(I) from aqueous waste, Sep. Sci. Technol., 54 (2019) 860–875.
[12] J.-K. Moon, K.-W. Kim, C.-H. Jung, Y.-G. Shul, E.-H. Lee, Preparation of organic-inorganic composite adsorbent beads for removal of radionuclides and heavy metal ions, J. Radioanal. Nucl. Chem., 246 (2000) 299–307.
[13] M.K. Jha, R.R. Upadhyay, J.-C. Lee, V. Kumar, Treatment of rayon waste effluent for the removal of Zn and Ca using Indion BSR resin, Desalination, 228 (2008) 97–107.
[14] X. Zhao, X.H. Bu, T. Wu, S.-T. Zheng, L. Wang, P.Y. Feng, Selective anion exchange with nanogated isoreticular positive metal-organic frameworks, Nat. Commun., 4 (2013) 2344.
[15] A.J. Cairns, J.A. Perman, L. Wojtas, V.C. Kravtsov, M.H. Alkordi, M. Eddaoudi, M.J. Zaworotko, Supermolecular building blocks (SBBs) and crystal design: 12-connected open frameworks based on a molecular cubohemioctahedron, J. Am. Chem. Soc., 130 (2008) 1560–1561.
[16] H.-R. Fu, Z.-X. Xu, J. Zhang, Water-stable metal–organic frameworks for fast and high dichromate trapping via single-crystal-to-single-crystal ion exchange, Chem. Mater., 27 (2014) 205–210.
[17] A.A. Alqadami, M. Naushad, Z.A. Alothman, A.A. Ghfar, Novel metal–organic framework (MOF) based composite material for the sequestration of U(VI) and Th(IV) metal ions from aqueous environment, ACS Appl. Mater. Interfaces, 9 (2017) 36026–36037.
[18] J.H. Park, Z.U. Wang, L.-B. Sun, Y.-P. Chen, H.-C. Zhou, Introduction of functionalized mesopores to metal–organic frameworks via metal–ligand–fragment coassembly, J. Am. Chem. Soc., 134 (2012) 20110–20116.
[19] H. Chang, M. Fu, X.-J. Zhao, E.-C. Yang, Four benzimidazole-based Zn^{II}/Cd^{II} polymers extended by aromatic polycarboxylate coligands: synthesis, structure, and luminescence, J. Coord. Chem., 63 (2010) 3551–3564.
[20] E. Şahin, S. İde, M. Kurt, Ş. Yurdakul, Structural investigation of dibromobis(benzimidazole)Zn(II) complex, J. Mol. Struct., 616 (2002) 259–264.
[21] R.M. Silverstein, G.C. Bassler, Spectrometric identification of organic compounds, J. Chem. Educ., 39 (1962) 546.
[22] M.S. Nair, R.S. Joseyphus, Synthesis and characterization of Co(II), Ni(II), Cu(II) and Zn(II) complexes of tridentate Schiff base derived from vanillin and DL-α-aminobutyric acid, Spectrochim. Acta, Part A, 70 (2008) 749–753.
[23] H. Temel, Ü. Çakir, B. Otludil, H.İ. Uğraş, Synthesis, spectral and biological studies of Mn(II), Ni(II), Cu(II), and Zn(II) complexes with a tetradentate Schiff base ligand. Complexation studies and the determination of stability constants (Ke), Synth. React. Inorg. Met.-Org. Chem., 31 (2001) 1323–1337.
[24] H. Long, P.X. Wu, N.W. Zhu, Evaluation of Cs^+ removal from aqueous solution by adsorption on ethylamine-modified montmorillonite, Chem. Eng., 225 (2013) 237–244.
[25] R.M. Cornell, Adsorption of cesium on minerals: a review, J. Radioanal. Nucl. Chem., 171 (1993) 483–500.
[26] M.R. Awual, S. Suzuki, T. Taguchi, H. Shiwaku, Y. Okamoto, T. Yaita, Radioactive cesium removal from nuclear wastewater by novel inorganic and conjugate adsorbents, Chem. Eng., 242 (2014) 127–135.
[27] M.R. Awual, T. Suzuki, T. Taguchi, H. Shiwaku, Y. Okamoto, T. Yaita, Selective cesium removal from radioactive liquid waste by crown ether immobilized new class conjugate adsorbent, J. Hazard. Mater., 278 (2014) 227–235.
[28] T. Yousefi, S. Yavarpour, S.H. Mousavi, M. Torab-Mostaedi, R. Davarkhah, H.G. Mobtaker, $FeIII_x$ $SnII_y$ $SnIV_{1-x-y}$ $H_n[P(Mo_3O_{10})_4]\cdot xH_2O$ new nano hybrid, for effective removal of Sr(II) and Th(IV), J. Radioanal. Nucl. Chem., 307 (2016) 941–953.
[29] N. Zhang, T. Kawamoto, Y. Jiang, A. Takahashi, M. Ishizaki, M. Asai, M. Kurihara, Z. Zhang, Z.F. Lei, D. Parajuli, Interpretation of the role of composition on the inclusion efficiency of monovalent cations into cobalt hexacyanoferrate, Chem. Eur. J., 25 (2019) 5950–5958.
[30] H.A. Alamudy, K. Cho, Selective adsorption of cesium from an aqueous solution by a montmorillonite-prussian blue hybrid, Chem. Eng. J., 349 (2018) 595–602.
[31] H.I. Adegoke, F. AmooAdekola, O.S. Fatoki, B.J. Ximba, Adsorption of Cr(VI) on synthetic hematite (α-Fe_2O_3) nanoparticles of different morphologies, Korean J. Chem. Eng., 31 (2014) 142–154.
[32] R. Salehi, M. Arami, N.M. Mahmoodi, H. Bahrami, S. Khorramfar, Novel biocompatible composite (chitosan-zinc oxide nanoparticle): preparation, characterization and dye adsorption properties, Colloids Surf., B, 80 (2010) 86–93.
[33] M.R. El-Naggar, M. Amin, Impact of alkali cations on properties of metakaolin and metakaolin/slag geopolymers: microstructures in relation to sorption of ^{134} Cs radionuclide, J. Hazard. Mater., 344 (2018) 913–924.
[34] R. Saberi, Y. Es-Hagh, S. Azad, A. Rajabi, Comparison of cesium adsorption behavior of CHCF-PAN, MnO_2-PAN, STS-PAN,

CM-PAN and AMP-PAN synthesized composites from aqueous solution, Desal. Water Treat., 107 (2018) 207–217.
[35] H.-R. Yu, J.-Q. Hu, Z. Liu, X.-J. Ju, R. Xie, W. Wang, L.-Y. Chu, Ion-recognizable hydrogels for efficient removal of cesium ions from aqueous environment, J. Hazard. Mater., 323 (2017) 632–640.
[36] R. Awual, Ring size dependent crown ether based mesoporous adsorbent for high cesium adsorption from wastewater, Chem. Eng., 303 (2016) 539–546.
[37] A.K. Kaygun, M. Eral, S.A. Erenturk, Removal of cesium and strontium using natural attapulgite: evaluation of adsorption isotherm and thermodynamic data, J. Radioanal. Nucl. Chem., 311 (2017) 1459–1464.
[38] S. Fan, J. Tang, Y. Wang, H. Li, H. Zhang, J. Tang, Z. Wang, X. Li, Biochar prepared from co-pyrolysis of municipal sewage sludge and tea waste for the adsorption of methylene blue from aqueous solutions: kinetics, isotherm, thermodynamic and mechanism, J. Mol. Liq., 220 (2016) 432–441.
[39] R.M. Ali, H.A. Hamad, M.M. Hussein, G.F. Malash, Potential of using green adsorbent of heavy metal removal from aqueous solutions: adsorption kinetics, isotherm, thermodynamic, mechanism and economic analysis, Ecol. Eng., 91 (2016) 317–332.
[40] K.-Y. Lee, M.S. Park, J.M. Kim, M. Oh, E.-H. Lee, K.-W. Kim, D.-Y. Chung, J.-K. Moon, Equilibrium, kinetic and thermodynamic study of cesium adsorption onto nanocrystalline mordenite from high-salt solution, Chemosphere, 150 (2016) 765–771.
[41] K.Y. Foo, B.H. Hameed, Insights into the modeling of adsorption isotherm systems, Chem. Eng. J., 156 (2010) 2–10.
[42] S. Rangabhashiyam, N. Anu, M.S. Giri Nandagopal, N. Selvaraju, Relevance of isotherm models in biosorption of pollutants by agricultural byproducts, J. Environ. Chem. Eng., 2 (2014) 398–414.
[43] M.J. Temkin, V. Pyzhev, Recent modifications to Langmuir isotherms, Acta Phys. Chim. Sin., 12 (1940) 217–222.
[44] A.K. Vipin, B. Hu, B. Fugetsu, Prussian blue caged in alginate/calcium beads as adsorbents for removal of cesium ions from contaminated water, J. Hazard. Mater., 258 (2013) 93–101.
[45] A. Nilchi, R. Saberi, M. Moradi, H. Azizpour, R. Zarghami, Adsorption of cesium on copper hexacyanoferrate–PAN composite ion exchanger from aqueous solution, Chem. Eng. J., 172 (2011) 572–580.